STM JOURNALS

Journal of
Polymer & Composites

ISSN: 2321-2810 (Online)
ISSN: 2321-8525 (Print)
Volume 11, Special Issue 12, 2023
DOI (Journal): 10.37591/JoPC

http://engineeringjournals.stmjournals.in/index.php/JoPC/index

Research JoPC

Investigations Into the Mechanical and Thermal Properties of Fe3C Compound: A Comprehensive Analysis

Purushotham Endla[1,*], Endla Akhil Balaji[2]

Abstract

This study focuses on investigating the mechanical properties of Fe3C powder using Williamson-Hall analysis, with a specific emphasis on employing the Mechanical Alloying Method (MAM). The main objective is to explore lattice strain (LS) and particle size (PS) in Fe3C prepared via MAM, with an expectation that the repetitive mechanical crushing process will lead to a reduction in LS while simultaneously decreasing particle size. Through the application of X-Ray Diffraction (XRD) techniques, parameters such as LS, particle size, Debye temperature (DT), Debye-Waller factor (DWF), and amplitude of vibrations (AV) of Fe3C are calculated and analyzed. Moreover, the study extends to the incorporation of the synthesized ferrite powders into polymer matrices to assess their potential applications in composite materials. This comprehensive analysis involves a detailed investigation into the mechanical and thermal properties of the composite materials. By evaluating these properties, the study aims to provide insights into the feasibility and effectiveness of utilizing Fe3C powder in polymer composites, thereby expanding the understanding of its potential applications in various engineering fields.

Keywords: Fe3C, XRD, SEM, particle size, lattice strain, Debye-Waller factor and vacancy formation energy.

INTRODUCTION

In recent years, there has been a surge in research endeavors aimed at synthesizing nanocomposites, driven by their unique scientific properties and considerable potential for various technological applications. Nanocomposites have emerged as a dynamic area of research due to their exceptional properties and diverse applications across various fields. These materials consist of a combination of powder or nanofillers dispersed within a matrix material, resulting in enhanced performance characteristics compared to traditional composite materials. The unique properties of nanocomposites stem from the synergistic effects between the nanofillers and the matrix material, offering tailored mechanical, thermal, electrical, and optical properties.

The synthesis of nanocomposites involves precise control over the dispersion and interaction of powder within the matrix material, often requiring innovative fabrication techniques. Researchers utilize a range of methods such as solution mixing, melt blending, in situ polymerization, and electrospinning to achieve homogeneous dispersion and maximize the potential of nanofillers.

In aerospace and automotive industries, nanocomposites offer lightweight yet durable alternatives for structural components, improving fuel efficiency and performance. In electronics, nanocomposites enable the development of miniaturized devices with enhanced conductivity and thermal management. Moreover, in biomedical applications, nanocomposites exhibit biocompatibility and drug delivery capabilities,

***Author for Correspondence**
Purushotham Endla

[1]Associate Professor, Department of Physics, School of Sciences, SR University, Hanamakonda, Telangana, India
[2]Student, Computer Science and Engineering, Kakatiya Institute of Technology and Science, Hanamakonda, Telangana, India

Received Date: January 03, 2024
Accepted Date: March 08, 2024
Published Date: April 01, 2024

Citation: Purushotham Endla, Endla Akhil Balaji. Investigations Into the Mechanical and Thermal Properties of Fe3C Compound: A Comprehensive Analysis. Journal of Polymer & Composites. 2023; 11(Special Issue 12): S225–S234.

promising advancements in tissue engineering and regenerative medicine.

Despite the progress made in nanocomposite research, challenges remain in achieving uniform dispersion, maintaining stability, and scaling up production for industrial applications. Additionally, understanding the effects of powder morphology, size, and surface chemistry on the properties of nanocomposites is crucial for tailoring their performance to specific application requirements.

In this context, this study aims to explore the synthesis, characterization, and potential applications of nanocomposites, employing advanced techniques to achieve enhanced properties and address current challenges. Through interdisciplinary collaboration and innovative approaches, nanocomposites hold the promise of revolutionizing various industries and driving forward technological innovation.

Sathiyavimal et al. [1] demonstrated the preparation of copper oxide, Jamzad et al. [2] and Ansari et al. [3] explored the iron oxide nanoparticles and Devatha et al. [4] iron nanoparticles synthesized unveiling their effectiveness at different proportions. Previous studies, Sadhasivam et al. [5] and Atta et al. [6] have extensively investigated various methods for synthesizing nanocomposites. Vasantharaj et al. [7], Vasantharaj et al. [8], Jamzadet al. [9] discussed different methods, Suddin et al. [10] discussed total design of polymer composite automotive bumper fascia. Salgado et al. [11] and Kirdat et al. [12] processed the effect of phenolic compounds on the synthesis of iron nanoparticles. Šutka et al. [13] identified precursor nanoparticles containing iron, crucial for thermal, Demirezen et al. [14] and Azizi [15] synthesis of Fe_3O_4 nanoparticles and their application. Nabati et al. [16] explored the synthesis of iron oxide. Alabdallah et al. [17] synthesized metal oxide nanoparticles. Concurrently, research has delved [18–19] into the realm of metal carbides, notably iron and iron carbide. These materials are esteemed for their exceptional properties, including high melting points and hardness, making them indispensable in applications such as cutting tools, wear-resistant components, and coatings.

Traditionally, the production of metal carbides involves high-temperature processes conducted in controlled atmospheres, typically within ceramic frameworks. However, this study diverges from convention by targeting the synthesis of room-temperature nanocrystalline variants of metal carbides. Our approach primarily employs mechanical alloying (MA) under inert conditions, a solid-state method renowned for its ability to produce high-quality nanocrystalline structures.

Focusing specifically on the Fe-C system, MA holds promise for yielding materials with outstanding properties spanning hardness, wear resistance, toughness, and magnetic characteristics. While prior research has predominantly centered on Fe3C and the formation of hexagonal carbides, certain aspects such as microstructural characteristics, lattice strain, and the influence of the Debye-Waller factor remain largely unexplored in this context. This study seeks to address these gaps in understanding and unlock the full potential of nanocrystalline metal carbides synthesized via MA.

This study's primary objective is synthesizing nanopowder of metalcarbide through high-energy ball milling at room temperature. The specific goals encompass determining particle size and investigating the impact of lattice strain on the Debye-Waller factor, employing advanced characterization techniques, such as X-ray diffraction (XRD), and quantitative analysis methods like Hall-Williamson analysis. Furthermore, Transmission Electron Microscopy (TEM) assesses crystallite size. XRD holds particular significance in this research as it furnishes comprehensive information that transcends the limitations inherent to TEM. Exploring the Debye-Waller factor assumes critical importance in unraveling lattice dynamics, particularly in the context of size and strain effects. Prior research endeavors have indeed investigated the impact of strain on Debye-Waller factors in diverse materials [20–24]. However, this study systematically examines lattice parameters, particle size, and the consequential impact of strain on Debye-Waller factors in Fe3C metal powder generated through ball milling. This comprehensive investigation offers original and profound insights into the intricate relationships among these crucial parameters. In sum, this research constitutes a well-conceived and

comprehensive endeavor, encompassing the synthesis and thorough characterization of Fe3C compound.

EXPERIMENTAL METHOD

Fe3C powder is divided into two parts: one part was used to prepare the initial sample, and the other part underwent a milling process in a ball mill for various durations (2,4, 6, 8 and 10 hours) to induce strains in the material.

To analyze the crystalline structure of the samples, the researchers recorded X-ray diffractograms for the initial sample and for each sample obtained after different milling times. The X-ray source emitted filtered CuKα radiation, and the goniometer was set to rotate the samples at a speed of 0.5 degrees per minute. The chart speed was adjusted to 20 mm per minute to capture the diffraction patterns in the 2θ range from 20 to 120 degrees.The XRD patterns obtained from the experiments are shown in Figure 1, which provides valuable information about the crystallographic characteristics and structure of the Fe3C samples after milling. The goniometer speed was set at 0.5º per minute with a chart speed of 20 mm/min. The measurements were carried out under room temperature conditions, with thermal diffuse scattering corrections applied following Chipman and Paskin's method [25]. Figure 1 shows the X-Ray diffraction pattern of Fe_3C.

METHOD OF ANALYSIS

The Debye-Waller theory [26, 27], describes the relationship between the mean square displacement of atoms in a crystal lattice and various parameters such as Debye temperature and atomic mass [28].

$$B = \frac{6h^2}{Mk_B\theta_M} W(X) \tag{1}$$

where h is the Planck's constant, k_B the Boltzmann constant, M the atomic weight. The function W(X) [28] is given by

$$W(X) = \frac{\phi(X)}{X} + \frac{1}{4}$$

Lattice Strain and Particle Size Determination

According to Bharati et al. [29] and Wilson [30], the total peak broadening B_r may be expressed as,

$$B_r = \frac{k\lambda}{t\cos\theta} + \varepsilon \tan\theta \tag{2}$$

which can be written as [31]

$$B_r \cos\theta = \frac{k\lambda}{t} + \varepsilon \sin\theta \tag{3}$$

The recorded half-widths were adjusted for instrument-related broadening, referencing a strain-free silicon powder. The particle size evolution over milling time remains within experimental error limits. This underscores that milling introduces strains significantly, while also impacting particle size measurably. Figure 2 illustrates a representative Hall-Williamson plot for Fe3C after 8 hours of milling time.

RESULTS AND DISCUSSION

The Fe3C powder, produced through high-energy ball milling for 10 hours, exhibited a significant reduction in crystalline size. The Debye Temperature parameter plays a crucial role in understanding the material's vibrations and thermal behavior, providing valuable insights into Fe3C's dynamic properties. Additionally, mean-square amplitudes of vibration values offer information on particle movement within the crystal lattice, shedding light on the material's structural dynamics. Regarding mechanical properties, lattice strain, particle size, vacancy formation energy, and lattice parameters

have been calculated and detailed in Table 1. It's observed that as milling time increases, lattice parameters (a and c) also increase. In terms of thermal properties, the Debye-Waller factor and Debye temperature have been analyzed. With increasing milling time, the Debye-Waller factor and mean-square amplitude of vibration increase, while the Debye temperature value decreases. This trend suggests that the Debye-Waller factor is crucial for understanding lattice vibrations and thermal vibrations in the crystal structure

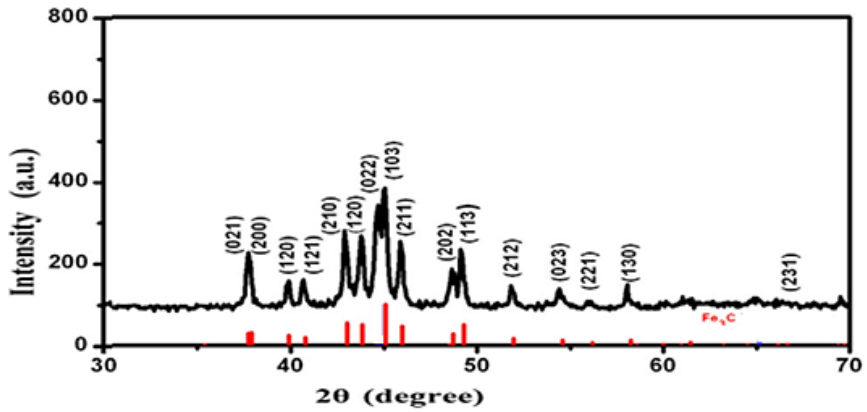

Figure 1. X-ray powder diffraction patterns of Fe3C.

Determining the lattice parameters is fundamental for characterizing the crystal structure of the synthesized nanoparticles, as they define the unit cell dimensions. The measurement of particle size is crucial in assessing the effectiveness of the synthesis process and understanding the materials' nanoscale properties. Lattice strain analysis provides valuable insights into the structural integrity of the nanoparticles, including any deviations from the ideal crystal lattice. Estimating vacancy formation energies for Fe3C nanoparticles is noteworthy; all the calculated values were added in Table 1. Vetelino et al. [32] attribute differences between calculated and experimental Debye-Waller factors to neglecting TDS corrections. Repeated

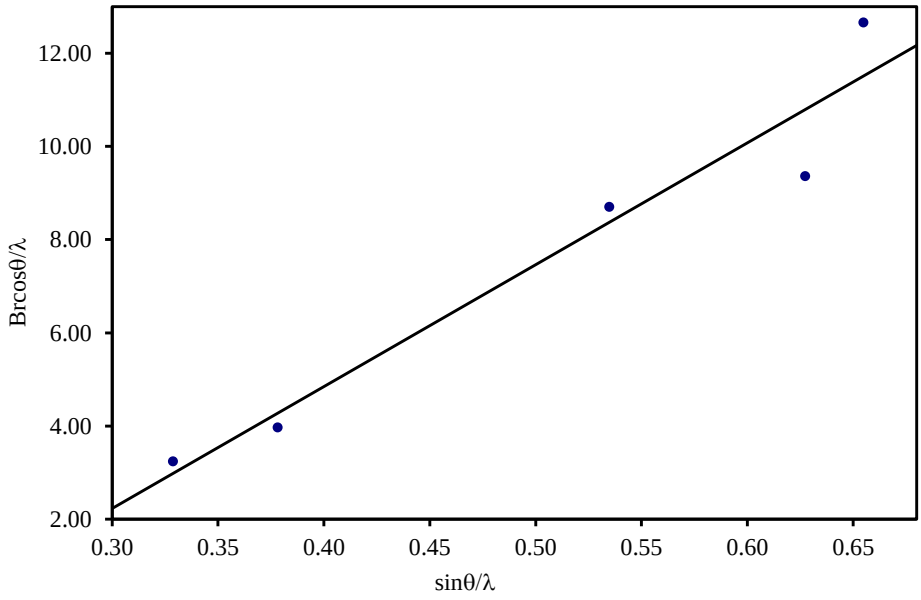

Figure 2. Plot of $B_r\cos\theta/\lambda$ Vs $\sin\theta/\lambda$ for Fe3C after milling for 16 hours.

Table 1. Calculated values of present work

Metal	Milling time (hrs)	ε x 10^3	t(nm)	a (nm)	b (nm)	c (nm)	<u>,	B(Å^2)	θ_M(K)	E_f(eV)

α–Fe C Fe_3C	0 0 0	0.8225 0.9903 1.1526	139.23 192.28 198.67	0.2866 0.2740 0.5091	--- --- 0.6743	--- 0.6707 0.4526	--- --- 0.0063	0.36 --- 0.30	428 --- 274	---- --- 5.86
Fe_3C	2	3.4129	11.12	0.5078	0.6792	0.4532	0.0076	0.46	223	3.74
Fe_3C	4	6.6233	5.36	0.5080	0.6785	0.4515	0.0083	0.69	182	2.65
Fe_3C	6	8.9521	4.56	0.5096	0.6784	0.4521	0.0098	0.93	163	1.89
Fe_3C	8	10.0433	4.49	0.5077	0.6794	0.4521	0.0147	1.05	149	1.46
Fe_3C	10	11.7536	4.49	0.5076	0.6795	0.4521	0.0241	1.22	128	0.82

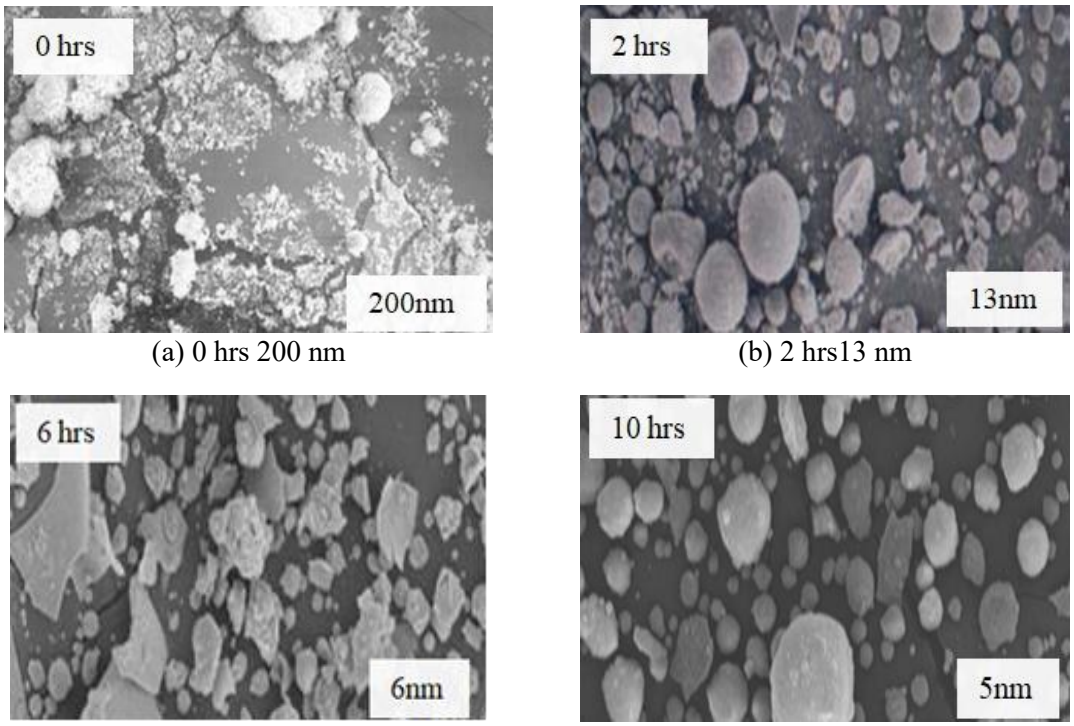

(a) 0 hrs 200 nm (b) 2 hrs13 nm

(c) 6 hrs 6 nm (d) 10 hrs 5 nm

Figure 3. (a-d) The SEM morphology of nanoparticles (a) 0 hours, (b) after 2 hours, (c) after 6 hours and (d) after 10 hours of milling of Fe3C powder.

The SEM morphology analysis yielded valuable insights into the particle sizes of the synthesized nanoparticles. The obtained particle size values from the Hall-Williamson method closely matched the SEM measurements, demonstrating good agreement between the two techniques. For the sample milled for zero hours, the Hall-Williamson method yielded a particle size of 198.67 nm, closely aligned with the SEM measurement of 200 nm. In the case of the sample milled for 4 hours, the Hall Williamson analysis provided a particle size of 5.36 nm, which closely matched the SEM measurement of 6 nm. Lastly, for the sample subjected to 10 hours of milling, the Hall-Williamson method estimated a particle size of 4.49 nm, which showed good agreement with the SEM measurement of 5 nm. This alignment between the Hall Williamson method and SEM measurements underscores the reliability and accuracy of the particle size assessments, reinforcing the robustness of the experimental findings regarding particle size reduction duringthe high-energy ball milling process.

Figure 4 explains that as the milling time increases from 0 to 10 hours, the particle size decreases significantly. This trend indicates that prolonged high-energy ball milling leads to a progressive reduction in the size of the Fe3C nanoparticles, resulting in finer and smaller particles.

Figure 5 shows the relationship between milling time and lattice strain of Fe3C nanoparticles. This phenomenon suggests prolonged high-energy ball milling induces more significant structural deformation and stress within the Fe3C nanoparticles. The increase in lattice strain is likely due to the

mechanical forces and collisions experienced by the particles during milling, leading to lattice distortions and defects due to the milling process.

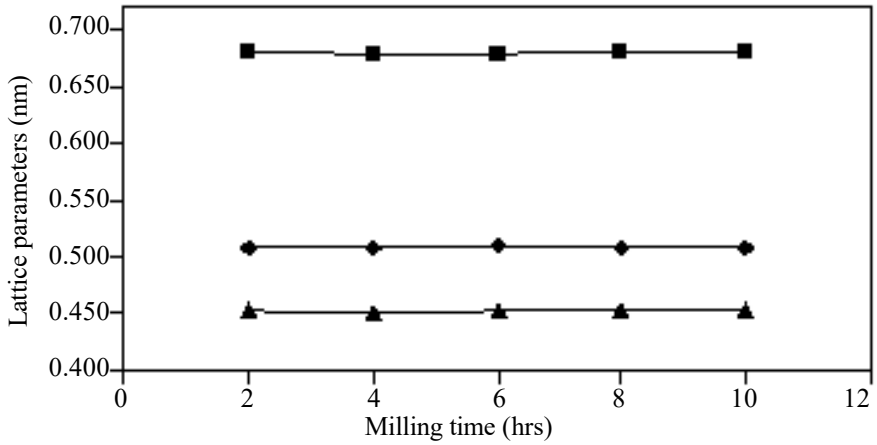

Figure 4. Plot between milling time and lattice parameters of Fe3C.

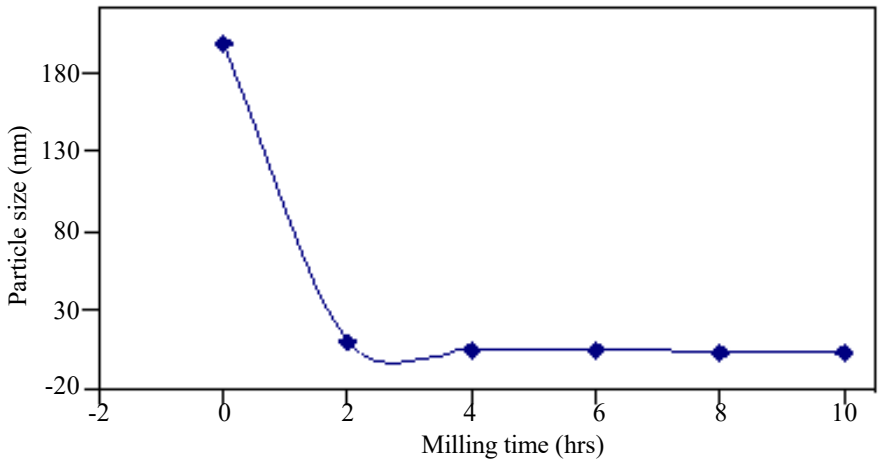

Figure 5. Plot between of milling time and particle size(t) of Fe3C.

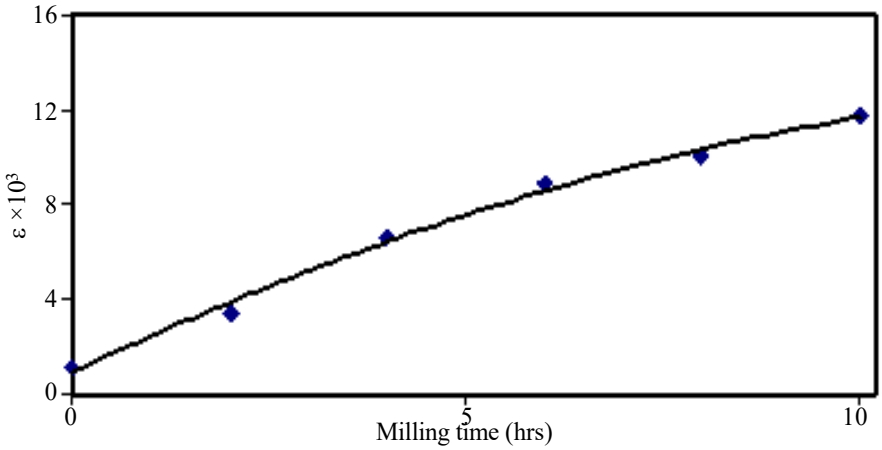

Figure 6. Plot between milling time and lattice strain of Fe_3C.

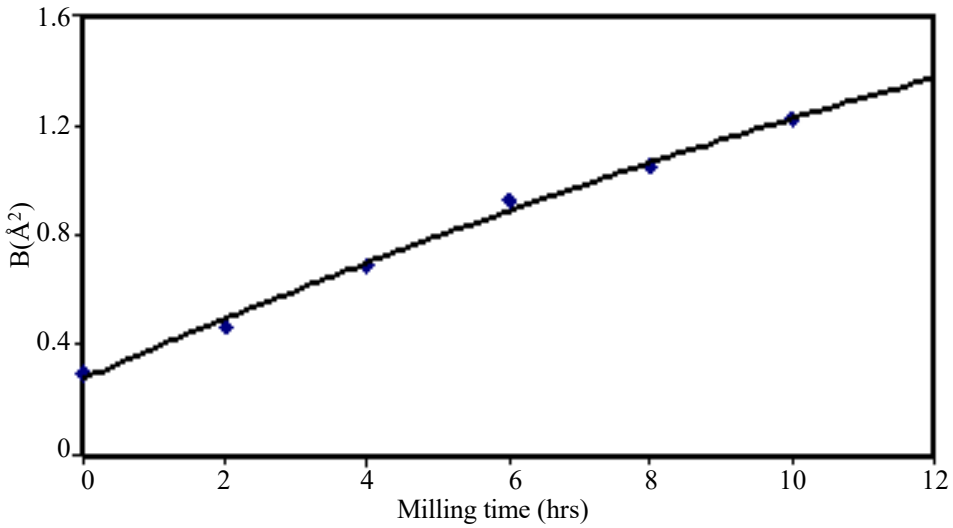

Figure 7. `Plot of milling time vs Debye-Waller factor of Fe3C.

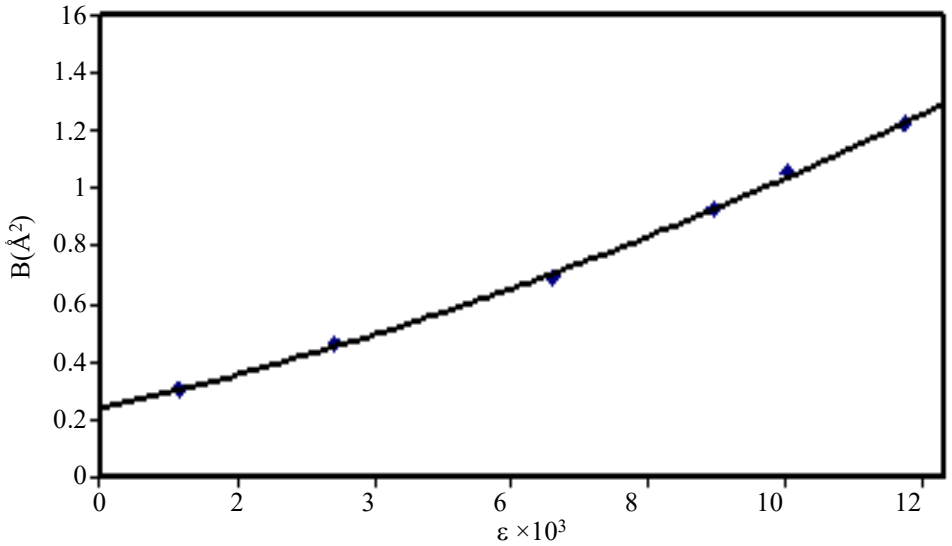

Figure 8. Plot of lattice strain vs Debye-Waller factor (B) of Fe3C.

In Figure 6, the plot depicts the relationship between milling time and the Debye-Waller factor of Fe3C nanoparticles. As the milling time increases from 0 to 10 hours, the Debye-Waller factor also increases, rising from 1.3 to 1.22 Å2. The increased Debye-Waller factor reflects the higher atomic mobility and structural disturbances resulting from the mechanical forces and energy imparted during the milling process, contributing to enhanced lattice disorder and thermal vibrations.

Figure 7 shows, the relation between lattice strain and Debye Waller factor, this correlation can be explained by the fact that lattice strain measures the deformation and distortion within the crystal lattice. As lattice strain rises, it indicates that the crystal lattice is undergoing more significant structural alterations, leading to greater disorder within the lattice. This increased disorder results in higher thermal vibrations and dynamic atomic motion, as reflected by the higher Debye-Waller factor (B). The lattice strain-induced structural changes contribute to enhanced atomic mobility and thermal fluctuations, leading to the observed increase in the Debye-Waller factor.

Glyde [33] formulated a relationship between the energy of vacancy formation (Ef) and the Debye temperature (θ) of a solid, given by

$$E_f = A(k/\hbar)^2 M\theta^2 a^2 \quad (4)$$

Its validity was confirmed across various fcc, bcc, and hcp metals [34–39].

Applications

- Fe3C is vital in steel production, enhancing strength and hardness in structural materials.
- It's employed in cutting tools and machinery components for its exceptional wear resistance.
- Fe3C finds use in bearings and gears, ensuring durability and reliability in mechanical systems.
- Its ferromagnetic properties make Fe3C suitable for magnetic recording media and sensors.
- In catalysis, Fe3C demonstrates high activity and stability, facilitating various chemical processes.

Fe3C plays a crucial role across diverse engineering applications, from enhancing the mechanical properties of structural materials in steel production to providing exceptional wear resistance in cutting tools and machinery components. Its versatility extends to applications in magnetic recording media, bearings and gears, and catalysis, where its unique properties contribute to durability, reliability, and high activity in various industrial processes.

CONCLUSIONS

The study comprehensively analyzed Fe3C powder subjected to a 10-hour high-energy ball milling process. The examination of X-ray diffractograms at various milling stages revealed a consistent reduction in particle size, highlighting the efficacy of milling in producing finer Fe3C powder.

- Particle Size Reduction: Through a series of X-ray diffractogram examinations conducted at various milling stages, we observed a consistent reduction in particle size. This underscores the effectiveness of the ball milling process in producing increasingly fine Fe3C powder.
- Our study delved into the relationship between the energy required for vacancy formation and the extent of lattice strain. This analysis yielded crucial information on how lattice strain influences the material's properties, particularly concerning defect formation.
- Our research underscores the dynamic structural changes and property alterations that Fe3C undergo during high-energy ball milling. These findings contribute significantly to our understanding of how milling affects nanomaterials and open avenues for potential materials science and engineering applications.

This study showcases the impact of high-energy ball milling on Fe3C powder and highlights the broader implications of lattice strain on material properties.

REFERENCES

1. Sathiyavimal, S. *et al.* Green chemistry route of biosynthesized copper oxide nanoparticles using *Psidium guajava* leaf extract and their antibacterial activity and effective removal of industrial dyes. *J. Environ. Chem. Eng.* 9, 105033 (2021).
2. Jamzad, M. &Bidkorpeh, M. K. Green synthesis of iron oxide nanoparticles by the aqueous extract of *Laurus nobilis* L. leaves and evaluation of the antimicrobial activity. *J. Nanostruct. Chem.* 10, 193–201 (2020).
3. Ansari, M. A. & Asiri, S. M. M. Green synthesis, antimicrobial, antibiofilm and antitumor activities of superparamagnetic γ-Fe_2O_3 NPs and their molecular docking study with cell wall mannoproteins and peptidoglycan. *Int. J. Biol. Macromol.* 171, 44–58 (2021).
4. Devatha, C., Jagadeesh, K. & Patil, M. Effect of Green synthesized iron nanoparticles by *Azardirachta indica* in different proportions on antibacterial activity. *Environ. Nanotechnol. Monit. Manag.* 9, 85–94 (2018).
5. Sadhasivam, S., Vinayagam, V. & Balasubramaniyan, M. Recent advancement in biogenic synthesis of iron nanoparticles. *J. Mol. Struct.* 1217, 128372 (2020).
6. Atta, A.M., El-Mahdy, G.A., Al-Lohedan, H.A., and Ezzat, A.O. (2014). Synthesis and application

of hybrid polymer composites based on silver nanoparticles as corrosion protection for line pipe steel. *Molecules* 19: 6246–6262Murgueitio, E. *et al.* Green synthesis of iron nanoparticles: Application on the removal of petroleum oil from contaminated water and soils. *J. Nanotechnol.* 2018, 1–8 (2018).

7. Vasantharaj, S., Sathiyavimal, S., Senthilkumar, P., LewisOscar, F. & Pugazhendhi, A. Biosynthesis of iron oxide nanoparticles using leaf extract of *Ruellia tuberosa*: Antimicrobial properties and their applications in photocatalytic degradation. *J. Photochem. Photobiol. B Biol.* 192, 74–82 (2019).
8. Vasantharaj, S., Sathiyavimal, S., Senthilkumar, P., LewisOscar, F. & Pugazhendhi, A. Biosynthesis of iron oxide nanoparticles using leaf extract of *Ruellia tuberosa*: Antimicrobial properties and their applications in photocatalytic degradation. *J. Photochem. Photobiol. B Biol.* 192, 74–82 (2019).
9. Jamzad, M. &Bidkorpeh, M. K. Green synthesis of iron oxide nanoparticles by the aqueous extract of *Laurus nobilis* L. leaves and evaluation of the antimicrobial activity. *J. Nanostruct. Chem.* 10, 193–201 (2020).
10. M. N. Suddin, M. S. Salit, N. Ismail, M. A. Maleque, and S. Zainuddin, "Total design of polymer composite automotive bumper fascia," *Suranaree Journal of Science and Technology*, vol. 12, pp. 39–45, 2004
11. P. Salgado, K. Márquez, O. Rubilar, D. Contreras, and G. Vidal, "The effect of phenolic compounds on the green synthesis of iron nanoparticles (FexOy-NPs) with photocatalytic activity," *Applied Nanoscience*, vol. 9, pp. 371–385, 2019.
12. Kirdat, P. *et al.* Synthesis and characterization of ginger (*Z. officinale*) extract mediated iron oxide nanoparticles and its antibacterial activity. *Mater. Today Proc.* 43, 2826–2831 (2021).
13. A. Šutka, M. Vanags, A. Spule et al., "Identifying iron-bearings nanoparticles precursor for thermal transformation into the highly active hematite photo-fenton catalyst," *Catalyst*, vol. 10, p. 778, 2020.
14. D. A. Demirezen, S. Yilmaz, and D. D. Yilmaz, "Green synthesis and characterization of iron nanoparticles using aesculus hippocastanum seed extract," *International Journal of Advances in Science Engineering and Technology*, vol. 6, 2 pages, 2018.
15. Azizi, A. Green synthesis of Fe3O4 nanoparticles and its application in preparation of Fe3O4/cellulose magnetic nanocomposite: A suitable proposal for drug delivery systems. *J. Inorg. Organomet. Polym. Mater.* 30, 3552–3561 (2020).
16. Nabati Souha, L., Alebrahim, M. T., Habibi Yangjeh, A. &Feizpoor, S. Green synthesis of iron oxide nanoparticles (Fe_3O_4) by extract of aerial organs of Russian knapweed (Acroptilon repens L.). *Cell. Mol. Res. (Iranian J. Biol.* (2021).
17. Alabdallah, N. M. *et al.* Green synthesized metal oxide nanoparticles mediate growth regulation and physiology of crop plants under drought stress. *Plants* 10, 1730 (2021).
18. Noor, R. *et al.* Comparative analysis of iron oxide nanoparticles synthesized from ginger (Zingiber officinale) and cumin seeds (Cuminum cyminum) to induce resistance in wheat against drought stress. *Chemosphere* 292, 133201 (2022).
19. M.Inagaki, H. Furuhashi, T.Ozeki et al., J Mater Sci.6,1520 (1971).
20. M.Inagaki, H.Furuhashi, T.Ozeki&S.Naka, J.Mater, Sci.8,312 (1973).
21. D.B.Sirdeshmukh, K.G.Subhadra, K.A.Hussain, N.Gopi Krishna, B.Raghave-ndra Rao, Cryst.Res.Technol, 28,15 (1993)
22. N.Gopi Krishna and D.B.Sirdeshmukh, Indian J Pure & Appl Phys.31, 198 (1993).
23. N.Gopi Krishna et al., Indian J Phys. 84(7), 887 (2010).
24. D.R.Chipman and A.Paskin,J.Appl. Phys. 30,1938 (1959).
25. N.Gopi Krishna, D.B.Sirdeshmukh, B.Rama Rao, B.J.Beandry and K.A.Jr.Gsch-neidner,Indian J Pure & Appl Phys.24, 324 (1986).
26. R.W.James, The optical principles of the diffraction of x-rays (Bell and Sons, London, 1967).
27. International tables for X ray crystallography, Vol.III(Kynoch press, Birmingham) (1968).
28. Bharati, R., Rehani, P.B., Joshi, Kirit N., Lad and Arun Pratap, *Indian Journal of Pure and Applied*

Physics, 44, (2006) 157–161.
29. Wilson, A.J.C.,(1949).X-rayOptics(Methuen, London).
30. Kaelble, E.F., *Handbook of X-rays* (New York Mc Graw ill) (1967)
31. J.F.Vetelino, S.P.Gaur, S.S.Mitra, Phys. Rev. B5, 2360 (1972).
32. H.R.Glyde, J.Phys and Chem Solids (G.B), 28, 2061 (1967).
33. Micro-and Macro-Properties of Solids, Springer Series in Material Science, (2006).
34. Purushotham, E. "Chemical Papers." Springer Nature, vol. 76, pp. 7327–7331, 2022.
35. Purushotham, E. "Evaluation of Debye temperatures of α-phase copper–zinc alloys by using X-Ray diffraction method." Materials Today Proceedings, vol. 46, no. 12, pp. 5922–5926, 2021
36. Purushotham, E. "Root mean square amplitudes of vibration and associated Debye temperatures of beryllium, scandium, and ruthenium." Materials Today: Proceedings, vol. 47, no. 15, pp. 5034–5037, 2021.
37. Purushotham, E., &Veerati Radhika. "Materials Today: Proceedings." Elsevier, vol. 47, no. 15, pp. 4993–4995, 2021.
38. Purushotham, E. "X-Ray Determination of Debye Temperature and Microhardness of Some Hexagonal Close Packed Elements Re, Os and Tl." IOP Conference Series: Materials Science and Engineering, vol. 1119, p. 012001, 2021.
39. Purushotham, E. "Characterization of size-dependent thermal properties in strained nanocrystalline powder using Williamson-Hall." IOP Conference Series: Materials Science and Engineering, vol. 981, p. 022086, 2020.

